

REVIEWS OF TOPICAL PROBLEMS PACS number: **76.30. – v**

Electron spin resonance in two-dimensional electron systems

A.V. Shchepetilnikov, I.V. Kukushkin

DOI: https://doi.org/10.3367/UFNe.2023.12.039626

Contents

Abstract. The main experimental studies of the spin properties of two-dimensional electron systems by means of electrically detectable electron spin resonance are discussed. The key aspects of spin resonance are considered, including the detection mechanism, the anisotropy of spin splitting, and the influence of hyperfine and spin-orbit interactions on the physics of spin resonance. Particular attention is paid to systems with strong electron-electron interactions formed in various AlAs/AlGaAs and ZnO/MgZnO semiconductor heterostructures. It is in such material systems that a whole series of unique physical phenomena related to spin have been observed. The prospects of electron spin resonance in two-dimensional systems are discussed.

Keywords: semiconductor heterostructures, two-dimensional systems, spin physics, electron spin resonance, transport properties

1. Introduction

The internal degrees of freedom of charge carriers significantly enrich the condensed matter physics and give rise to both a huge variety of ground states of electron and hole systems [1–4] and a nontrivial spectrum of excitations [5–7]. The most striking example of such a degree of freedom is spin. From an applied point of view, the spin degree of freedom can be used in addition to the charge of an electron or hole for storing and processing information in the paradigm of innovative electronics.

A.V. Shchepetilnikov (*), **I.V. Kukushkin** (**)
Osipyan Institute of Solid State Physics, Russian Academy of Sciences,
ul. Akademika Osip'yana 2, 142432 Chernogolovka,
Moscow region, Russian Federation
E-mail: (*) shchepetilnikov@issp.ac.ru, (**) kukush@issp.ac.ru

Received 10 November 2023, revised 22 December 2023
Uspekhi Fizicheskikh Nauk **195** (1) 34 – 49 (2025)
Translated by V.L. Derbov

The spin has a quantum nature and is a pseudovector oriented in space, with its magnitude measured in units of $\hbar$ (the reduced Planck constant), and the proportionality factor S between the spin value and $\hbar$ takes only discrete values, integer or half-integer. The fundamental nature of the spin degree of freedom is emphasized by the fact that particles with integer and half-integer spin obey fundamentally different statistics, the Bose–Einstein or Fermi–Dirac distribution, respectively. In a system of charged fermions, the Coulomb interaction between particles, together with the Pauli exclusion principle, leads to the appearance of a new type of interaction, the exchange interaction. It is this type of interaction that determines the energy scale in a variety of magnetic systems [9–11]. For example, under certain conditions, strong interparticle interaction in an electron system can lead to a chain of phase transitions associated with the appearance of a macroscopically large spin polarization [3, 4]. Such a transition was predicted theoretically at the beginning of the 20th century and only recently was implemented experimentally in a series of ultrahigh-purity, low-density, two-dimensional electron systems [12, 13].

The spin degree of freedom of a particle is inextricably linked to the magnetic moment, the magnitude of which is proportional to the spin value. As a consequence, the application of an external magnetic field causes Larmor precession of the spin with a frequency $\mathbf{\Omega}$, generally given by the expression

$$\hbar\Omega_\alpha = g_{\alpha\beta}\mu_\mathrm{B}B_\beta\,. \tag{1}$$

Here, μ_B is the Bohr magneton, and B_β is the projection of the magnetic field vector onto the coordinate axis. The proportionality coefficient $g_{\alpha\beta}$ is usually called the Landé factor or g-factor. In free space (or a crystal with high symmetry), the g-factor is a scalar [14], but when the dimensionality is reduced, e.g., in two-dimensional electron systems, the Landé factor becomes a tensor [15], and the Larmor precession frequency begins to depend on the orientation of the external magnetic field in space [16].

The nonzero magnetic moment associated with the spin also provides the possibility of interaction between the spin degree of freedom and the translational motion of the electron in space. Such interaction is usually called spin-orbit coupling. For simplicity, let us consider the motion of a free electron in a constant external electric field. In accordance with Lorentz transformations, a magnetic field proportional to the vector product of the particle velocity and the electric field arises in the coordinate system of the electron itself. This field causes electron spin precession. The effect under consideration is relativistic and, therefore, weak. However, in real material systems, crystalline solids, or molecules, the electron moves in strong electric fields of the atomic cores, which significantly enhances the effect under consideration [17, 18]. In this case, all the main characteristics of the spin-orbit coupling become parameters of the material under study, such as the electron effective mass, and the precise determination of these parameters is a separate fundamentally important scientific problem. It should be emphasized that the spin-orbit coupling plays a key role in modern semiconductor spin physics, since it is a bridge between the motion of charges in a crystal and an internal degree of freedom, the spin. For example, such coupling offers opportunities for manipulating the spin state of an electron [19] and largely determines the relaxation rate of the nonequilibrium spin polarization of delocalized electrons [20, 21]. Moreover, strong spin-orbit coupling is one of the necessary conditions for the existence of unique quasiparticles — Majorana fermions — in hybrid semiconductor structures [22, 23].

The magnetic moment associated with the spin of an electron placed in a crystal can also interact with the moments of the lattice nuclei. Such interaction cannot be ignored in many solids, for example, in GaAs — a semiconductor of extreme importance for both fundamental science and applied physics — and the effective magnetic field of polarized nuclear spins, which leads to the energy splitting of electron states with different spin projections, can reach several teslas [24], which is quite comparable to typical external magnetic fields. Moreover, one of the main channels for the relaxation of electron spins localized in one or several quantum dots (essentially semiconductor spin qubits) is precisely the process of exchanging magnetic moments between electrons and nuclei [25].

The concept of a spin degree of freedom was formulated at the beginning of the 20th century, and its existence has been confirmed many times, e.g., in the Stern–Gerlach experiments [26]. It was shown that silver atoms have two possible discrete angular momenta, despite the complete absence of orbital momentum. The subsequent development of spin physics was accompanied by the emergence of new and increasingly sophisticated experimental techniques that make it possible to study even the most subtle spin phenomena. In the middle of the 20th century, the technique of electron paramagnetic (or spin) resonance (or ESR) [27] emerged, which played a key role in the development of many modern concepts of the spin properties in a variety of material systems: from macroscopic biological objects to nanoscale defects in crystals containing a single spin.

ESR is based on the phenomenon of resonant absorption of electromagnetic radiation, provided that the energy of its quanta coincides with the magnitude of the energy splitting of electron states with different spin projections and the magnetic moment conservation law is fulfilled. In this case, the absorption of radiation can be detected directly, e.g., by the deterioration of the quality factor of a microwave resonator. This approach works well even for systems with reduced dimensionality under conditions of a relatively small number of spins [28]. On the other hand, the absorption of radiation can modify the physical properties of the electron system itself, e.g., optical or transport properties. In the first case, we speak of optical detection of spin resonance [29], and in the second case, of electrical detection [30].

The purpose of this review is to present the main experimental results in the field of studying the spin properties of two-dimensional electron systems using the technique of electrically detected spin resonance. The presentation is organized as follows. Section 2 describes the main experimental implementations of the approach and considers possible detection mechanisms. Section 3 discusses the study of the g-factor and its anisotropy in various semiconductor heterostructures. Section 4 presents experimental studies of the spin-orbit coupling using the electron spin resonance technique. Section 5 presents the main experimental results on hyperfine interactions between the spins of electrons and nuclei of the crystal lattice in semiconductor heterostructures. Section 6 discusses the physics of spin in strongly correlated two-dimensional electron systems. Section 7 outlines the prospects of electron spin resonance in two-dimensional systems.

2. Method of electrical detection of spin resonance in two-dimensional systems

2.1 Experimental method

As a rule, electron spin resonance is registered by the resonant absorption of electromagnetic radiation, the frequency of which corresponds to the splitting energy between the states of an electron with different spin projections [31]. Under certain conditions, the dissipation of wave energy in an electron system leads to a change in the resistance of the sample under study. Thus, the sample itself can act as an effective bolometric detector of resonant absorption of electromagnetic radiation, and the ESR will be observed as a peak in the resistance of the sample. This approach has proven itself in studying the spin properties of two-dimensional electron systems at low temperatures in quantizing magnetic fields.

To carry out low-temperature transport measurements, as a rule, samples are made in the form of standard Hall bar with a drain, a source, and several potentiometric contacts. A typical view of a Hall bar is shown in Fig. 1c. An electric current is passed through the drain–source, and the voltage, proportional to either the longitudinal or transverse resistance of the two-dimensional electron channel, is measured at the potentiometric contacts. A typical view of R_{xx} and R_{xy} of a two-dimensional electron system is shown in Fig. 1a. The transport characteristics demonstrated were obtained in a GaN/AlGaN heterostructure at a temperature of 0.5 K. More detailed experimental studies of this sample, including the use of the spin resonance technique, are given in Ref. [32]. As a rule, experiments on ESR spectroscopy of two-dimensional systems are carried out at low temperatures (down to several ten mK) and in high magnetic fields. The quality of the structures under study is quite high and usually allows one to observe well-expressed Shubnikov–de Haas oscillations and the quantum Hall effect under such conditions.

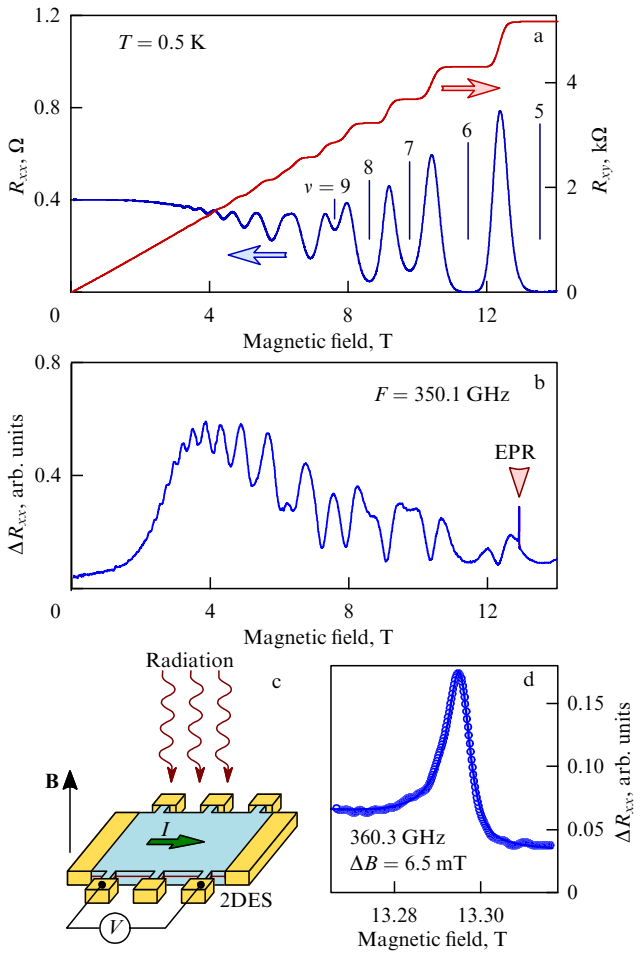

Figure 1. (a) Typical longitudinal and transverse resistance of a Hall bar at low temperatures ($T = 0.5$ K) and in high magnetic fields. The sample is a GaN/AlGaN heterojunction. (b) Variation of the longitudinal magnetoresistance of the sample due to absorption of electromagnetic radiation with a frequency of 350.1 GHz. Data were obtained using the same sample as in panel a. Arrow marks position of ESR. (c) Typical circuit for electrical detection of ESR in a two-dimensional system. (d) Example of an ESR peak measured in a GaN/AlGaN heterojunction at incident radiation frequency of 360.3 GHz. Temperature was 0.5 K.

With such a measurement scheme, the ΔR_{xx} signal in the region of low magnetic fields is usually determined by the plasma response of the system [33]. In this case, the energy of plasma waves excited by the incident radiation dissipates in the electron system and thereby heats it. In quantizing magnetic fields, ΔR_{xx} exhibits oscillatory behavior, which is explained by the dependence of the Shubnikov–de Haas oscillation amplitude on temperature [34]. As a rule, the spin resonance peak has a significantly smaller width than all other features of ΔR_{xx}, which makes possible high-precision measurements of its main characteristics: the amplitude, width, and resonance value of the magnetic field.

The conductivity of a two-dimensional channel can also be measured in a noncontact manner, e.g., by the transmission of a coplanar waveguide deposited on the sample surface [35]. In this case, spin resonance can also be measured in a noncontact manner [36]. We emphasize that other transport properties of the system also change near resonance, which brings additional possibilities for detecting spin resonance. For example, ESR can be detected by photovoltage [37] generated at the contacts to a two-dimensional system, as well as by a resonant change in tunnel characteristics [38]. Transport approaches to ESR detection work well not only for two-dimensional systems but also for zero-dimensional objects, such as quantum dots [39].

Let us consider another important methodological aspect of ESR in two-dimensional systems. As a rule, the transition associated with ESR is magnetic dipole, i.e., the maximum absorption of the maximum wave energy should be observed in the antinode of the alternating magnetic field. This behavior was observed in GaAs/AlGaAs heterostructures [40]. However, many studies have suggested that the spin flip near ESR can also be induced by an alternating electric field of the wave [41–43]. Indeed, the electric field causes an oscillating correction to the electron wave vector at the same frequency, which is 'processed' into an alternating magnetic field, with which the electron spin interacts. Experimental evidence of the electric-dipole nature of ESR was obtained in studies of AlAs and InAs quantum wells [44, 45]. Due to the key role of spin-orbit coupling in this mechanism, the ratio of the contributions from the electric and magnetic-dipole transitions near ESR depends on the characteristics of a particular material [46].

2.2 Electron spin resonance in quantum Hall effect regime

Let us discuss in more detail the mechanism of changing the longitudinal resistance in a two-dimensional channel under the action of electromagnetic radiation near spin resonance in the quantum Hall effect regime. For simplicity, we will restrict ourselves to the case of weak interaction between electrons in a two-dimensional system. In a high magnetic field perpendicular to the plane of a two-dimensional system at low temperatures (it is under such conditions that spin resonance spectroscopy usually occurs), the spectrum of electron motion is a discrete set of Landau levels, each split by spin projections. Each sublevel has a finite number of states in which electrons can be, and the number of filled sublevels is called the filling factor ν.

Let us consider the simplest case of an electron system having a unity filling factor, when the lowest spin sublevel of the zero Landau level is completely filled, and the upper sublevel is empty. Then, the spin resonance is absorption of photons incident on the electron system, accompanied simultaneously by the transition of electrons from the lower to the upper sublevel with the flip of the electron spin. The excited electron and the hole left at the lower sublevel form a bound state — a spin exciton, the dispersion of which was calculated theoretically in a number of papers [47, 48] and is shown schematically in Fig. 2. In full accordance with the Larmor theorem, the exciton energy begins with single-particle Zeeman splitting, grows quadratically with respect to the wave vector k, and in the limit of large k asymptotically tends to the value of the exchange energy $e^2/\epsilon l_b$. Here, $l_b = \sqrt{\hbar c/eB}$ is the magnetic length, and ϵ is the relative permittivity of the medium. In the act of absorption of a photon, the laws of conservation of both energy and momentum must be satisfied. Due to the large wavelength of light compared to the value of l_b for typical magnetic fields, the dispersion curves of the photon and spin exciton intersect at $kl_b \sim 10^{-4} - 10^{-5}$, i.e., the dependence of the spin exciton energy on the wave vector can be disregarded. As was shown in Ref. [48], the characteristic radius of the exciton is kl_b^2, which means that only compact excitations are created near the spin resonance. Note that the dispersion of the spin exciton can be measured by Raman scattering [50] rather

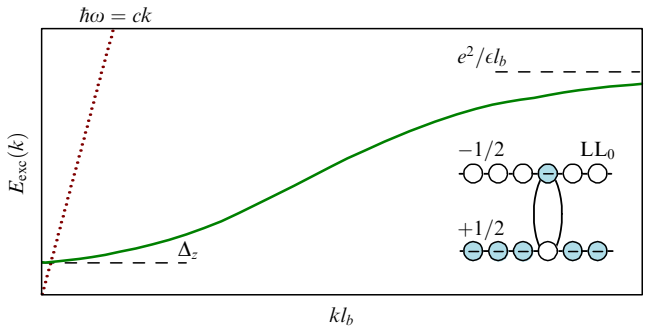

Figure 2. Schematic representation of spin exciton dispersion near unity filling factor. Dotted line shows dispersion of light. Dispersions of spin exciton and photon intersect at $kl_b \ll 1$. Inset schematically shows spin exciton formation near unity filling factor. Theoretical calculations were performed in Refs [47, 48].

than direct absorption of radiation. In Refs [51, 52], spin excitons with a large k were excited via interaction with surface acoustic waves, which made it possible to measure the evolution of the short-wave part of the spin exciton spectrum depending on the filling factor and clearly demonstrate its relationship with the exchange energy.

Let us now turn to the key question for understanding the mechanism of transport detection of spin resonance: how can spin excitons excited by light affect the transport properties of the system? Indeed, a spin exciton with a small k is a compact and electrically neutral particle, and therefore cannot participate in transport. Only excitons with a large wave vector can participate in charge transfer processes. At large k, the size of the spin exciton increases due to the Lorentz force. When its size becomes large enough and comparable to the characteristic free path (for example, with the characteristic fluctuation length of a random potential), the exciton can be expected to decay into independent electrons and holes, which can participate in charge transport. This is, notably, illustrated by the well-known fact that the activation energy of a quantum Hall ferromagnet near a unity filling factor is significantly greater than the single-particle Zeeman energy [53–55]. Thus, light-excited spin excitons can affect the resistance of a two-dimensional channel only indirectly, transferring energy to all spin excitons, including those with large k. We emphasize that, as a rule, the lifetime of spin excitons at low temperatures and in high magnetic fields is large [56, 57] and exceeds the characteristic energy relaxation time by several orders of magnitude, which means that most of the created excitations manage to increase the temperature of the entire ensemble of spin excitons by ΔT, while in the linear approximation the resistance of a two-dimensional channel should change by an amount proportional to $\Delta T \delta R_{xx}/\delta T$.

The mechanism described above is confirmed by measurements of the temperature dependence of the spin resonance amplitude [49, 58, 59]. The experimentally obtained amplitude is compared with the first derivative of the longitudinal resistance of the sample, measured independently. When the value of the single-particle spin splitting is much greater than the experimental temperature, very good agreement between these two dependences is observed, which is illustrated in Fig. 3 using the example of a wide AlAs quantum well. As was shown in Ref. [58], when the spin splitting is not too large (e.g., in GaAs/AlGaAs heterostructures), due to the smallness of the Landé factor, the amplitude and the first derivative behave similarly only in the region of low temperatures, and at a temperature higher than the spin splitting, a decrease in the amplitude relative to the derivative is observed. This feature is associated with a decrease in the number of vacant states at the upper spin sublevel due to thermal fluctuations. In Ref. [49], it was also demonstrated that the above mechanism is not entirely valid when moving away from odd filling factors.

3. Spin resonance and Landé factor in two-dimensional systems

3.1 Landé factor in a magnetic field

The Landé factor is a coefficient of proportionality between the energy of the spin splitting of electron states and the magnitude of the magnetic field and, in fact, is the most important parameter in spin physics. Thus, the thermodynamics of a quantum Hall ferromagnet near odd filling

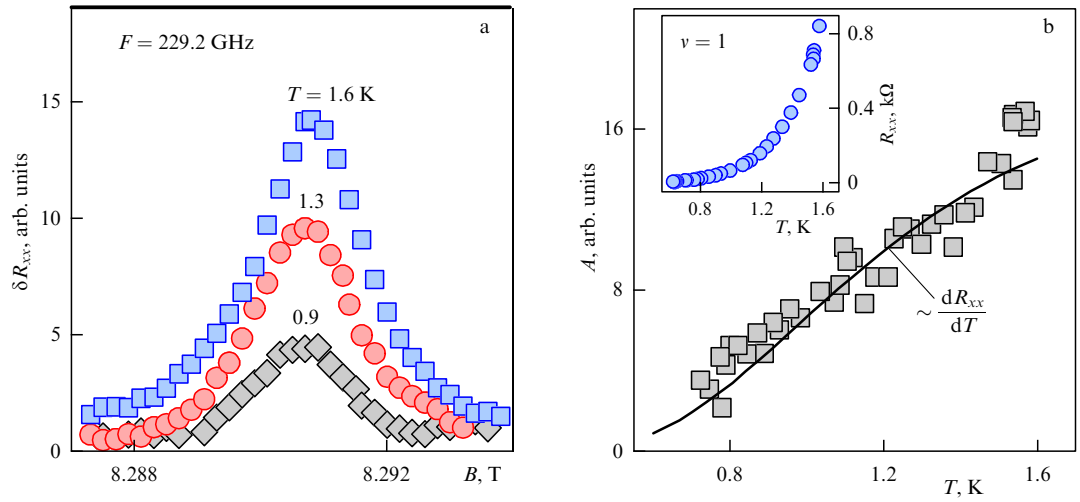

Figure 3. Typical ESR peaks observed at different temperatures in a wide AlAs quantum well near unity filling factor. (b) Dependence of spin resonance amplitude (symbols) on temperature near unity filling factor for the same sample. Solid line specifies course of first derivative of resistance of two-dimensional channel with respect to temperature. Derivative was extracted independently from temperature dependence of the sample (shown in inset). Derivative was normalized to coincide with ESR amplitude in high-temperature region. More detailed experimental data are given in Ref. [49].

factors is determined precisely by single-particle Zeeman splitting, i.e., the g-factor [60]. Moreover, the sign of g specifies the orientation of the spin relative to the magnetic field and, thus, controlling the magnitude and sign of the Landé factor will allow us to control the spin state of the electron.

It is well known that the value of the g-factor for a free electron is ≈ 2 and is isotropic in space. However, in crystalline media, as a rule, the value of the Landé factor is significantly modified due to the presence of spin-orbit coupling and is a parameter of the medium, which is specified by the band structure of the material [14]. Thus, in some narrow-band semiconductors (e.g., InAs, GaSb) the spin-orbit coupling effectively mixes valence p-states into the conduction band, and g can reach values of up to -10 and more [61]. Thus, it is an important fundamental problem to determine the Landé factor in various semiconductors and heterostructures based on them.

The ESR technique allows accurate measurement of the Landé factor, since ESR resonance lines are usually characterized by a high quality factor, which means that the position of the magnetic field B_0 of the resonance line at a fixed frequency of incident radiation F can be determined with very high accuracy. The value of the Landé factor can then be easily calculated:

$$g = \frac{hF}{\mu_B B_0}\,. \tag{2}$$

It should be emphasized that such an expression for the Landé factor does not at all imply a linear dependence of the ESR frequency on the magnetic field. Moreover, in some semiconductor heterostructures, a quadratic dependence of F on the magnetic field is observed. Such nonlinear effects have been studied in detail using ESR in various GaAs/AlGaAs heterostructures containing a two-dimensional electron system.

Figure 4 shows the dependence of the ESR frequency and the Landé factor calculated according to Eqn (2) on the magnetic field for a GaAs/AlGaAs heterojunction with a two-dimensional electron density of $n = 1.5 \times 10^{11}$ cm^{-2}. The data were obtained at a sample temperature of 1.3 K [62]. The arrows indicate the position of the filling factors.

Note two important features of the demonstrated data, which are typical of all two-dimensional electron systems enclosed in GaAs/AlGaAs heterostructures. Near each odd ν, the $g(B)$ dependence is linear, and the slope of the line depends on the ν value itself. It was shown experimentally in [63] that the slope tangent is directly proportional to ν. From the theoretical point of view, such behavior is a consequence of the nonparabolicity of the GaAs conduction band, which was demonstrated in Ref. [64]. In this paper, it was also shown that the proportionality coefficient between the slope tangent of the $g(B)$ line and ν is determined by the band structure of the material system. Let us emphasize that the linearity of $g(B)$ is preserved even under conditions of the fractional quantum Hall effect, and the appearance of energy gaps in the spectrum of a two-dimensional system near fractional states does not affect the $g(B)$ dependence. This experimental fact was reported in Ref. [40].

Linear extrapolation of the measured dependences $g(B)$ into the region of zero magnetic fields makes it possible to obtain the value of g_0, the single-particle Landé factor near the bottom of the dimensional quantization subband. As a rule, the approximation is carried out by magnetic field dependences of the Landé factor near different odd filling factors simultaneously, which significantly increases the accuracy of the determined value. The values of g_0 obtained in this way coincide very well with the values of the Landé factor determined using other experimental approaches: the Raman scattering spectroscopy [65] and magneto-optical experiments to measure the angle of rotation of light polarization [66].

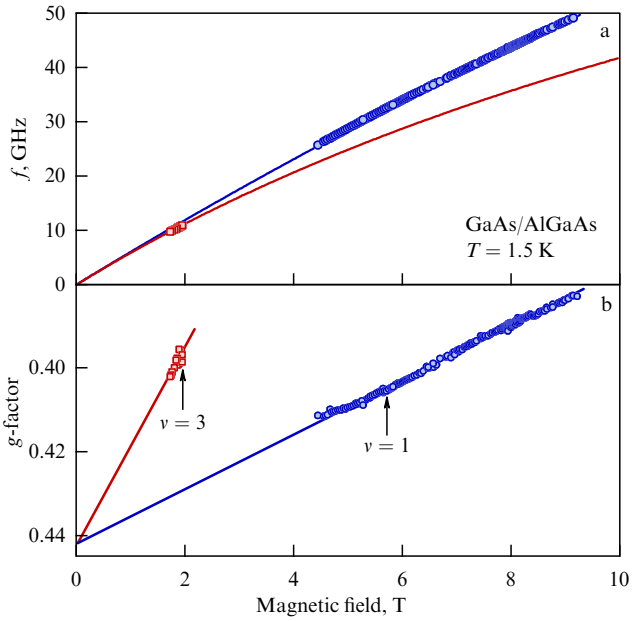

Figure 4. Magnetic field dependences of resonance frequency (a) and Landé factor (b), measured in a GaAs/AlGaAs heterojunction with density $n = 1.5 \times 10^{11}$ cm^{-2} in a perpendicular field. Arrows indicate positions of filling factors 1 and 3.

The ESR technique made it possible to measure with high accuracy the dependence of g_0 on various parameters of GaAs/AlGaAs heterostructures, namely, the quantum well width and the Al concentration in the barrier layers [67, 68]. A decrease in the well width led to a decrease in the absolute value of the Landé factor, which is explained by two factors: a decrease in the admixture of p-states into the conduction band due to an increase in the energy of dimensional quantization of the structure, as well as an increase in the square of the electron wave function in barrier layers with a different g_0 value. In Ref. [69], the possibility of limited control of the g-factor by applying an external electric field to the heterostructure was demonstrated. In this case, the electric field in some sense acts similarly to a decrease in the well width — it pushes the electron wave function into the barrier and changes the levels of dimensional quantization of the electron. In a series of studies [70–72], the g-factor of an electron in single-layer graphene was measured using the ESR technique. It was shown in [72] that the value of g strongly depends on the composition of the layers surrounding the graphene.

3.2 Anisotropy of Landé factor

The value of the Landé factor in two-dimensional electron systems enclosed in various semiconductor heterostructures may depend not only on the amplitude but also on the direction of the magnetic field. The ESR technique has shown itself most clearly in the study of this effect in GaAs

and AlAs heterostructures. Let us consider the main results of these studies in more detail.

Bulk semiconductors GaAs and AlAs have a zinc blende structure characterized by the point symmetry group T_d. The high symmetry of such materials imposes very strong restrictions on the form of the tensor g, which lead to degeneration of the $g_{\alpha\beta}$-factor into a scalar. In this case, the Zeeman splitting does not depend on the direction of the magnetic field. A two-dimensional electron system has a reduced symmetry, which gives rise to anisotropy of the spin splitting in space [15, 73–75]. Note that the symmetry properties of the structure largely depend on the crystallographic direction of the growth axis. Below in this section, all samples considered will have the growth axis [001].

Quantum wells grown symmetrically along the [001] direction have the point group D_{2d}. In this case, the Landé factor is symmetric in the plane of the structure, and $g_{\alpha\beta}$ has two independent components, $g_{\parallel}$ and g_{zz}. If the profile of the quantum well confining potential is asymmetric along the growth direction of the heterostructure, then such a system is characterized by the group C_{2v}. In this case, $g_{\alpha\beta}$ has three independent components and, as a consequence, anisotropy of the spin splitting appears in the plane of the structure. Note that the mechanism for the appearance of in-plane anisotropy is closely related to the existence of spin-orbit coupling in the electron band of the semiconductor. The in-plane component of the magnetic field mixes the motion of an electron along the growth direction (the spectrum of such motion is a set of size quantization levels) and in the plane of the structure. The resulting correction to the in-plane quasi-momentum of the electron changes the effective spin-orbit magnetic fields, which leads to anisotropy of the spin splitting in the plane of the well. The sequential consideration given in Ref. [16] allows us to write in the axes [100] (Ox), [010] (Oy), and [001] (Oz):

$$g_{yx} = g_{xy} = \frac{2\gamma e}{\hbar^3 c \mu_{\mathrm{B}}} \left(\langle p_z^2 \rangle \langle z \rangle - \langle p_z^2 z \rangle \right). \tag{3}$$

Here, γ is the Dresselhaus constant for the bulk material. The expression in parentheses in Eqn (3) vanishes for a structure symmetric along the growth direction. For an asymmetric structure, nondiagonal components appear in the $g_{\alpha\beta}$ tensor. Considering the initially selected axes, we can say that the principal axes of the $g_{\alpha\beta}$ tensor in the plane of the structure should be directed along the crystallographic axes [110] and [1$\bar{1}$0]. Note that the application of an external electric field also leads to a significant asymmetry of the electron wave function in the direction of structure growth and, therefore, modifies the in-plane components of the Landé factor tensor. This effect offers one more mechanism for controlling the electron g-factor.

The Landé factor was measured experimentally in [001] GaAs/AlGaAs heterostructures using the ESR technique in [67, 68, 76, 77]. Similar results were obtained using the magneto-optical technique based on the analysis of the rotation of the plane of polarization of incident light [66, 78–82]. In the ESR technique, the dependence $g(B)$ was first measured for different orientations of the magnetic field, after which extrapolation to the zero field made it possible to extract the value of the Landé factor for a given field direction. The orientation of the field relative to the crystallographic axes of the sample can be conveniently chosen in accordance with the layout shown in Fig. 5a. In this case, θ is the angle between the magnetic field and the normal to the quantum well plane, and φ specifies the orientation of the in-plane component relative to [110]. Then, for a fixed φ, in accordance with Eqn (1), we can write

$$g^2 = g_{zz}^2 \cos^2\theta + g_{\parallel}^2 \sin^2\theta. \tag{4}$$

Thus, the dependence of g^2 on $\cos^2\theta$ should be linear, and its extrapolation to the region of $\cos\theta = 0$ (i.e. $\theta = 90°$) allows one to determine the in-plane component for a given φ. This fact is illustrated in Fig. 5b for the cases of a GaAs

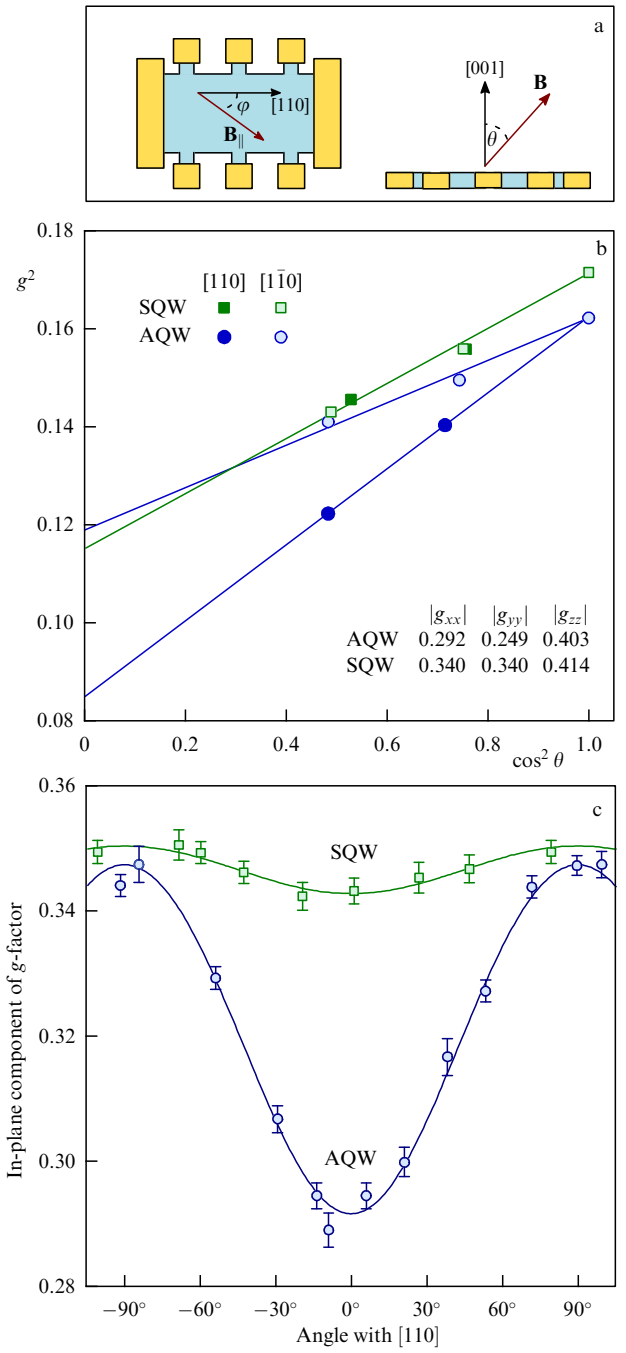

Figure 5. (a) Schematic diagram of magnetic field orientation relative to sample and its crystallographic directions. (b) Dependence of the square of g-factor on the square of cosine of tilt angle between external magnetic field and normal to sample plane for GaAs/AlGaAs quantum wells grown nominally symmetrical and asymmetrical. In-plane component is directed along one of the crystallographic axes [110] or [1$\bar{1}$0]. (c) Dependence of in-plane component of Landé factor on angle φ for same two structures.

quantum well symmetric and asymmetric along the growth direction in the case of $\varphi = 0^\circ$ and 90°. A more detailed description of experimental studies is given in Refs [76, 77]. Figure 5c shows the dependence of the in-plane component on the angle φ. It is clearly seen that, for a symmetric well, the anisotropy of the in-plane component of the Landé factor is clearly noticeable, while, for a symmetric well, the g-factor is practically isotropic in the plane (a small anisotropy is probably associated with the residual asymmetry of the structure growth). In [68, 83], an analysis of the anisotropy of the Landé factor was used to determine the Dresselhaus constant in GaAs. The resulting γ value differed several times from the result of calculations based on the GaAs band structure. Such a discrepancy is usually attributed to the occurrence of interface spin-orbit coupling [84–86]. The dependence of the slope of the magnetic field dependence $g(B)$ on the orientation of the magnetic field was studied in Refs [76, 77]. It was demonstrated that the g-factor is determined only by the magnetic field component perpendicular to the plane of the two-dimensional electron system. This feature fits well into the model in which the dependence of the Landé factor on the field is caused by the nonparabolicity of the conduction band. It is the perpendicular field that significantly modifies the spectrum of electron motion in the plane of the quantum well. The dependence of the Landé factor tensor and the pseudotensor of its derivatives with respect to the magnetic field on the width of the quantum well was measured in Ref. [67]. It was shown that a decrease in the well width suppresses the in-plane anisotropy of the g-factor, which is probably due to a decrease in the asymmetry along the growth direction of the structure in narrower quantum wells. In Ref. [87], the anisotropy of the Landé factor was measured in a wide AlAs quantum well. In such structures, electrons fill two equivalent in-plane valleys, the principal axes $g_{\alpha\beta}$ of which, due to the symmetry of the structure, are rotated relative to each other by $\Delta\varphi = 90^\circ$. As a consequence, the dependence of the in-plane component of g on φ has two branches shifted relative to each other by this value of $\Delta\varphi$.

4. Electron paramagnetic resonance and hyperfine interaction

In this section, we discuss the influence of the interaction between the magnetic moments of electrons and lattice nuclei on the physics of ESR in two-dimensional electron systems. On the one hand, such interaction provides an additional and very accurate tool for studying the spin properties of electrons. The change in the relaxation rate of nuclear spins can be used to judge the modification of the spectrum of spin excitations of the electron system [88], and analyzing the Knight shift of nuclear magnetic resonance allows measuring the spin polarization of electron systems. For example, measuring the Knight shift in GaAs/AlGaAs quantum wells made it possible to obtain evidence of the existence of topological spin-texture excitations near the unity filling factor [7] and showed that the unique state of the fractional quantum Hall effect near the filling factor of $5/2$ is completely spin polarized [89]. On the other hand, hyperfine interaction leads to dynamic polarization of nuclear spins near the spin resonance and, therefore, to the appearance of an Overhauser shift, which significantly distorts the shape and position of the spin resonance [90, 91].

Let us consider the spin part of the single-particle Hamiltonian of an electron in a magnetic field, considering the hyperfine interaction:

$$H = g\mu_B B_\alpha S_\alpha + A I_\alpha S_\alpha \,. \tag{5}$$

The left term describes Zeeman splitting; the right term describes the hyperfine interaction. Parameter A is the hyperfine interaction constant. As a rule, the dominant contribution is the Fermi contact interaction, and the value of A is proportional to the square of the electron wave function near the nucleus. In the general case, A is a tensor $A_{\alpha\beta}$, but, for the further discussion, this is not of fundamental importance and A can be considered a scalar. The hyperfine interaction Hamiltonian can be rewritten using the raising and lowering operators $I_\pm$ and $S_\pm$ in the form

$$H_{\rm hf} = A I_\alpha S_\alpha = 0.5(I_+ S_- + I_- S_+) + I_z S_z \,. \tag{6}$$

The expression in parentheses corresponds to the processes of simultaneous flip of the spin of the electron and nucleus with conservation of the total magnetic moment and is the basis of one of the relaxation channels for the nonequilibrium spin polarization in the electron system [56]. This process is shown schematically in Fig. 6a. Even though under typical experimental conditions this channel is not dominant in two-dimensional electron systems, some part of the nonequilibrium polarization of electrons created during the absorption of microwave radiation near the electron spin resonance relaxes into the nuclear subsystem. In this case, a nonzero average polarization of nuclei arises, i.e., $\langle I_z \rangle \neq 0$. Thus, near the electron spin resonance, dynamic polarization of nuclear spins occurs. The described phenomenon plays an important role in the physics of magnetic resonance phenomena, since it allows achieving sufficiently large values of $\langle I_z \rangle$. Consequently, the sensitivity of the nuclear magnetic resonance technique significantly increases [92].

On the other hand, the appearance of a nonzero $\langle I_z \rangle$ leads to a shift in the position of the spin resonance in the magnetic field by $B_{\rm N}$, the Overhauser shift [90]. Indeed, averaging Eqn (5) yields

$$hF = g\mu_B(B + B_{\rm N}) = g\mu_B\left(B + \frac{A\langle I_z \rangle}{g\mu_B}\right). \tag{7}$$

The Overhauser shift $B_{\rm N}$ is seen to be directly proportional to the average nuclear spin. Despite the apparent weakness of hyperfine interaction, this correction to the position of the electron spin resonance cannot always be disregarded. For example, in semiconductor systems, the observed ESR shifts reach several T [93] and are quite comparable to the applied external magnetic field.

The appearance of the contribution from nuclear spins to the single-particle spin splitting of electron states has important consequences. First, the Overhauser shift in combination with the effect of dynamic nuclear polarization significantly complicates ESR experiments in two-dimensional electron systems. Indeed, near the ESR, the nonzero $\langle I_z \rangle$ is arranged, dynamically shifting the resonance position of the ESR. If the directions of the external magnetic field change and the Overhauser shift are opposite (for example, the external field increases, and the Overhauser shift moves the ESR to the region of lower fields), then the resonance peak will have a smaller width and amplitude. If both the shift and the external field change in a similar way, i.e., the Overhauser shift 'catches up' with the external field, then the system is in

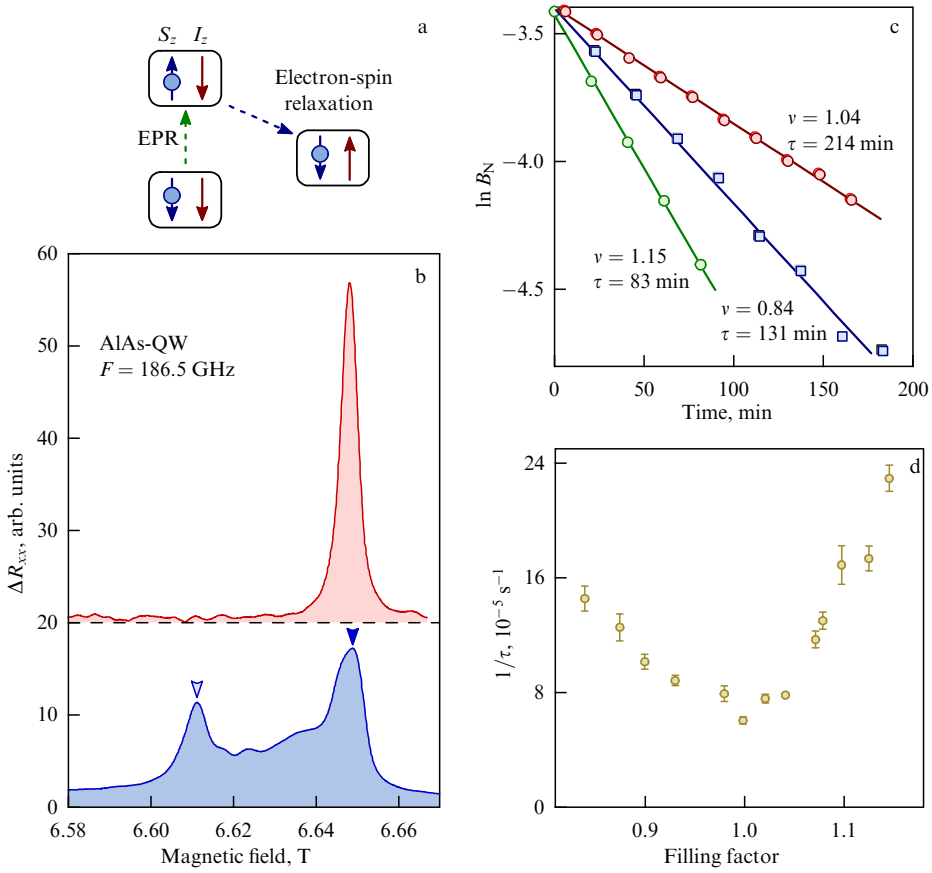

Figure 6. (a) Schematic representation of process of dynamic polarization of nuclei, in which part of nonequilibrium polarization of electron spins relaxes into nuclear subsystem. (b) Typical form of spin resonance near unity filling factor in a wide [001] AlAs/AlGaAs quantum well before (upper curve) and after (lower curve) dynamic polarization of nuclei. Data are shifted for clarity along vertical axis. (c) Overhauser decay with time near different filling factors of electron system in the same sample. Approximation of experimental data (symbols) by a linear dependence (straight lines) made it possible to determine relaxation time of nuclear spins. Obtained time is indicated near each data set. (d) Dependence of spin-lattice relaxation times of nuclei on filling factor of electron system. Data are given for the same sample.

spin resonance conditions for a long time. In this case, the resonance peak itself becomes extremely wide and no longer has a regular shape. This effect requires careful selection of the radiation power exciting the spin resonance, as well as the field reversal rate. Typical ESR peaks before and after nuclear spin polarization are shown in Fig. 6. The spin resonance peaks were measured in a wide [001] AlAs quantum well near a filling factor of 1 at a temperature of 1.4 K. It can be seen that, upon nuclear spin polarization, the ESR peak splits into several field-shifted peaks. In GaAs quantum wells, the ESR peak is usually shifted as a whole [91].

On the other hand, the hyperfine interaction opens up wide experimental possibilities for studying the spin properties of the nuclear subsystem. For example, the Overhauser shift of the spin resonance allows measuring the polarization of the nuclear subsystem. In Ref. [94], the polarization of nuclear spins created by optical pumping was estimated from the Overhauser shift. Relaxation of $\langle I_z \rangle$ leads to the attenuation of the Overhauser shift, which allows measuring the spin-lattice relaxation time of nuclei [95]. Such measurements, performed in a wide [001] AlAs quantum well, are presented in Ref. [96]; let us consider them in more detail. A typical change in the Overhauser shift of the spin resonance with time without additional pumping of nuclear spins is shown in Fig. 6c. The data are presented for a wide [001] AlAs quantum well at a temperature of 1.5 K. The decay of the Overhauser shift is exponential in time. The characteristic time of nuclear spin relaxation can be measured from the slope of the time dependence of the shift logarithm. The dependence of the inverse spin-lattice relaxation time $1/\tau$ on the filling factor of the system is shown in Fig. 6d for the same sample. It is clearly seen that $1/\tau$ is largely determined by the filling factor. Similar results were obtained earlier in GaAs/AlGaAs heterostructures [95]: the time $1/\tau$ demonstrated magnetic quantum oscillations upon filling factor variation. Thus, it can be concluded that the dominant channel of nuclear spin relaxation is based on the interaction between the spins of nuclei and of the electron system, and $1/\tau$ is determined by its spin state. In Ref. [97], it was shown that the formation of fractional quantum Hall effect states also slows down the relaxation of nuclear spins but does not affect the width of the electron spin resonance, i.e., the time of spin-spin relaxation in the electron system.

The coupling of electron and nuclear spins allows detecting nuclear magnetic resonance by the transport properties of a two-dimensional electron channel [91, 98, 99]. For this purpose, as a rule, the sample is placed in an additional coil, the axis of which is oriented in the plane of the two-dimensional system, and an alternating current passed through the coil creates an alternating magnetic field oscillating with the frequency of the current and directed perpendicular to the external magnetic field. Near nuclear magnetic resonance, nonzero spin polariza-

tion (it can be created, e.g., by the dynamic polarization of nuclei) is destroyed, which is detected by a change in the shape of the spin resonance. In this case, it is possible to fix the frequency of the radiation and change the magnetic field or fix the field and scan the frequency. Such a technique is rather accurate and allows, e.g., resolving the quadrupole splitting of the nuclear magnetic resonance line [96].

There is another method of electrical detection of nuclear magnetic resonance, which is usually applied at extremely low temperatures. At temperatures of ~ 10 mK, the spin splitting of nuclei in typical magnetic fields becomes comparable to the characteristic thermal energy kT. Then, thermal fluctuations do not completely suppress the average nuclear spin and $\langle I_z \rangle$ becomes nonzero, and a contribution proportional to $\langle I_z \rangle$ appears in the energy splitting of the electron spin states. At low temperatures near odd filling factors of the electron system, the resistance of the two-dimensional channel depends exponentially on the spin gap and even small variations in it, associated with a change in $\langle I_z \rangle$, lead to quite noticeable changes in the transport properties of the sample [100, 101]. Near nuclear magnetic resonance, the radio-frequency electromagnetic field resonantly destroys $\langle I_z \rangle$, which allows electrical detection of nuclear magnetic resonance [102, 103]. Such a technique, for example, made it possible to study in detail the spin properties of an electron system near various states of the fractional quantum Hall effect using the Knight shift of nuclear resonance [89, 104].

5. Electron spin resonance in systems with spin-orbit interaction

In this section, we consider the effect of spin-orbit coupling on the physics of spin resonance in two-dimensional electron systems. Spin-orbit interaction in the electron band couples the spin degree of freedom of electrons and their orbital motion in the plane of the system. Nonzero spin-orbit coupling of electron states is possible only in the absence of an inversion center in the system, which means that, in semiconductor heterostructures, it can arise due to the absence of an inversion center in the bulk materials of which the structure is composed, or due to the asymmetry of the structure itself. Local asymmetry of bonds at heteroboundaries also gives rise to spin-orbit coupling.

Let us first consider the influence of the spin-orbit coupling on the splitting of electron states by spin in strong quantizing magnetic fields. In this case, the energy spectrum will be a set of Landau levels, each of which is split by spin. The spin-orbit interaction can usually be considered a small correction in this case, and the formalism of perturbation theory can be used. We restrict ourselves to the case of the Dresselhaus spin-orbit coupling, linear in the wave vector, having the form $\beta(k_x\sigma_x - k_y\sigma_y)$. It is convenient to rewrite this expression through $k_\pm = k_x \pm \mathrm{i}k_y$ and $\sigma_\pm = (1/2)(\sigma_x \pm \mathrm{i}\sigma_y)$, since, in the symmetric gauge, $k_+ = \sqrt{2}a^+/l_b$ and $k_- = \sqrt{2}a/l_b$, where the operators a^+ and a are the operators of the electron transition between adjacent Landau levels without spin flip. Here, as before, l_b is the magnetic length. The total Hamiltonian of the electron will then have the form

$$H = \hbar\omega_c\left(a^+a + \frac{1}{2}\right) + g\mu_B B\sigma_z + \frac{\beta\sqrt{2}}{l_b}(a^+\sigma_+ + a\sigma_-)\,. \qquad (8)$$

Here, the quantity ω_c is the cyclotron frequency, and $\hbar\omega_c$ is the distance between adjacent Landau levels with the same spin projection. In fact, the spin-orbit interaction provides the possibility of transition between Landau levels with a spin flip of the electron. We can similarly rewrite the Rashba interaction linear in the wave vector: $\alpha(k_y\sigma_x - k_x\sigma_y)$. Then, using the second-order perturbation theory, we can find a correction to the Landé factor, which specifies the spin splitting of the Landau level with number N:

$$g - g_0 = C(\beta^2 - \alpha^2)\,\frac{2N+1}{B}\,. \qquad (9)$$

Here, the parameter C is a combination of world constants and material parameters of the system — the effective mass and Landé factor. The value of C is directly proportional to the effective mass of the electron, and the corresponding correction to the g-factor will be most significant in two-dimensional systems with a large effective mass of charge carriers. We also emphasize that the approximation used to derive Eqn (9) implies the smallness of the spin-orbit correction and is therefore applicable only in the region of high magnetic fields.

The electron spin resonance technique allows measuring the Landé factor with high accuracy and, as a result, extracting the correction specified in Eqn (9). Let us consider how this approach works using narrow AlAs quantum wells grown in the [001] direction as an example. The main experimental results of these studies are presented in [105–107]. Let us discuss them in more detail. Figure 7b demonstrates the experimentally obtained dependence of the g-factor on the magnetic field in a 5-nm AlAs quantum well grown in the [001] crystallographic direction. The characteristic magnetoresistance of a two-dimensional electron system enclosed in this structure is shown in Fig. 7a. As the magnetic field decreases, the electron g-factor near odd filling factors continuously increases and demonstrates pronounced jumps around each even filling factor. In this case, the value of the Landé factor itself directly at the odd filling factor $\nu = 2N + 1$ (here, as before, N specifies the Landau level number) demonstrates a clear dependence on ν. This behavior is fundamentally different from that typically observed in GaAs/AlGaAs heterostructures. Indeed, the small effective mass of the electron in GaAs, apparently, determines the smallness of the correction to the g-factor in Eqn (9).

Following Ref. [106], we demonstrate that the spin resonance technique makes it possible to determine the spin-orbit correction to the g-factor with high accuracy. For this purpose, Fig. 7c shows typical ESR lines measured near $\nu = 1.7, 3, 5,$ and 7, with the corresponding Landau level numbers $N = 0, 1, 2,$ and 3. For convenience, the magnetic field is normalized to the value $B_0 = hF/g_0\mu_B$ — its own for each ESR peak. The field B_0 represents the position of the spin resonance in the absence of spin-orbit renormalization of the g-factor. Then, the difference in the positions of the resonance peaks constructed in this way directly reflects the correction to the Landé factor in accordance with Eqn (9). The observed difference exceeds the width of the resonance lines, which allows measuring the indicated correction with high accuracy.

Near odd filling factors, the experimental dependence of the Landé factor on the magnetic field is very well approximated by expression (9) with a single fitting parameter, the coefficient β^2. The value of g_0 is taken from the region of high magnetic fields, where the spin-orbit correction can be ignored. In this case, the contribution from α^2, i.e., from the

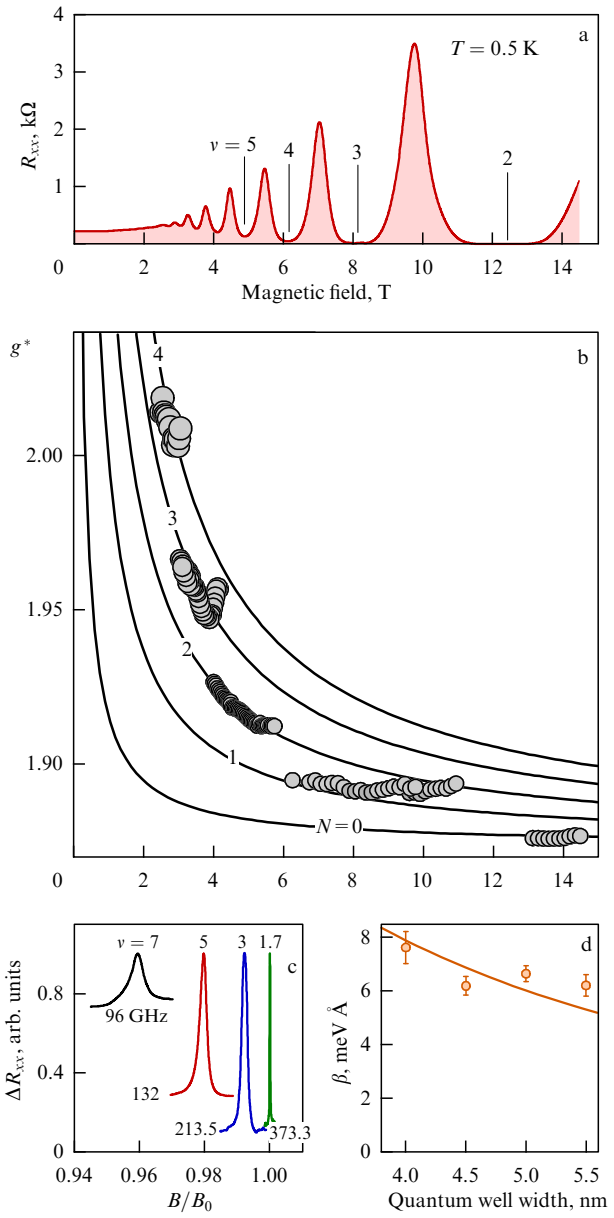

Figure 7. (a) Longitudinal resistance of wo-dimensional electron channel formed in a 5-nm [001] AlAs quantum well at 0.5 K. (b) Dependence of Landé factor on magnetic field near various odd filling factors $\nu = 2N + 1$. Symbols are experimental data obtained in a 5-nm [001] AlAs quantum well, solid lines are theoretical approximation using a single parameter β. Values of N are indicated near each curve. (c) Typical ESR peaks measured near different filling factors $\nu = 1.7, 3, 5, 7$. Frequencies of electromagnetic radiation F are indicated near each curve. Field is normalized to value $B_0 = hF/g_0\mu_B$ (individual for each peak). (d) Dependence of spin-orbit interaction constant β on quantum well width. Solid line is approximation of data taking into account theoretically calculated value of $\langle k_z^2 \rangle$.

Rashba-type spin-orbit coupling, is assumed to be negligibly small. To confirm this statement, measurements were performed in [105] in one-side doped samples with different electron concentrations in a two-dimensional system. Indeed, the coefficient α is proportional to the electric field E along the growth direction in the vicinity of the two-dimensional system. In the absence of an external electric field, a nonzero E is produced by the δ-layer of ionized donors separated from the well by a barrier layer. Since the structure as a whole is not charged, the value of E is proportional to the two-dimensional electron density n, hence, $\alpha \sim n$. This situation is quite typical of quantum wells [108]. The contribution to the g-factor associated with the Rashba interaction is then proportional to n^2 and opposite in sign to the contribution from the Dresselhaus interaction. Experimentally, the dependences of the g-factor coincided for different values of n, which determines the smallness of the Rashba interaction in narrow AlAs quantum wells. Figure 7d shows the dependence of the coefficient β on the width of the AlAs quantum well; in Ref. [106], an approximation of such a dependence considering the theoretically calculated value of $\langle k_z^2 \rangle$ made it possible to obtain a value of $\gamma \approx 3.5$ eV Å^3 in bulk AlAs.

As is clearly seen from Fig. 7b, two spin resonance peaks are observed near even filling factors, which clearly contradicts the expected zero spin polarization near even filling factors. We will discuss the possibility of observing spin resonance near even ν in the next section of this review.

The approach described above was also extended to other material systems. In Ref. [109], the Rashba spin-orbit coupling constant was measured in a series of GaN/AlGaN heterojunctions with different electron densities. Bulk GaN has a wurtzite structure, the presence of a high-order symmetry axis in which dictates the dominance of the Rashba-type spin-orbit coupling. The electron density in the samples was varied in diverse ways: by optical pumping, using an upper gate semitransparent to microwave radiation, and changing the Al concentration in the barrier layers. An analysis of the dependence of the constant on the electron density made it possible to establish the coefficients for the terms of the spin-orbit coupling, both linear and cubic in the wave vector. Similar measurements were made for a series of ZnO/MgZnO heterojunction samples with different Mg concentrations in the barrier layer in [110].

It is of interest to compare the obtained spin-orbit constants with the results of other techniques typically used to study spin-orbit interactions. Techniques based on the analysis of the beats in the Shubnikov–de Haas oscillations in the region of low magnetic fields, as a rule, give an overestimated result in comparison with the ESR spectroscopy technique [111], which is probably explained by the extreme sensitivity of the technique to inhomogeneities in a two-dimensional system [112]. On the other hand, the constants measured by the weak antilocalization effect demonstrate good agreement with the results of the ESR technique. This fact was shown in Ref. [109] considering the renormalization of the effective mass of electrons due to the electron-electron interaction. It should also be noted that in GaN/AlGaN heterojunctions the electron density is significantly higher than in AlAs quantum wells, which results in a significantly smaller contribution of electron-electron interaction to the transport properties of a two-dimensional system and, as a consequence, good agreement between the results of the two methods even without taking renormalizations into account.

In material systems with the energy spectrum linear in the wave vector, the spin-orbit coupling splits the spin resonance line into two with the same slope relative to the magnetic field [113]. An analysis of the relative position of these lines made it possible to determine the energy of the bulk spin-orbit splitting.

Let us dwell on one more important aspect. Strong spin-orbit coupling violates the Larmor theorem, which means that a multiparticle contribution may appear in the spin splitting measured by ESR spectroscopy [114, 115]. How-

ever, in none of experiments discussed in this section were such effects observed, which is probably due to the insufficient strength of the spin-orbit coupling.

6. Spin resonance in two-dimensional electron systems with strong electron-electron interaction

In the previous sections, we discussed the physics of the electron spin system in the single-particle approximation, i.e., we considered the system as a set of particles that do not interact with each other. In a number of cases, this approach is quite justified. However, under certain conditions, the exchange interaction arising from the usual Coulomb repulsion of charged fermions — the electrons — together with the Pauli exclusion principle, largely determines the spin properties of a two-dimensional system and contributes to the physics of electron spin resonance. This section of our review is devoted to a discussion of these effects.

Many-particle effects are especially pronounced when the kinetic energy of charged particles is much less than the characteristic energy of interaction between them. In this case, to describe the contribution from many-particle interaction, it is convenient to use the dimensionless parameter r_s, the ratio of the characteristic energy of Coulomb repulsion and the Fermi energy. Since the energy of interaction between electrons is inversely proportional to the average interparticle distance, i.e., $\sim n^{1/2}$, and the Fermi energy is proportional to the combination n/m^*, the parameter r_s will increase with decreasing effective electron mass. For example, if the ratio of the characteristic Coulomb energy to the Fermi energy reaches ~ 40, spontaneous spin polarization of a two-dimensional electron system occurs [4, 12, 13]. In this case, the characteristic value of n is only 10^{10} cm^{-2}. Such low electron densities, and with them Fermi energies, entail extremely stringent requirements for the purity of the electron system, since at ultra-low electron densities both decent transport characteristics and exceptional homogeneity of the system must be maintained.

A strong external magnetic field leads to the transformation of the continuous spectrum of electron motion into a discrete one — a set of Landau levels. In fact, the magnetic field 'freezes' the electron motion in the plane of a two-dimensional system. In this case, even in samples with quite average characteristics, one can observe quantum many-particle effects, for example, the fractional quantum Hall effect [116, 117], including states with even denominators [118], Wigner crystallization at filling factors less than unity [119], and a ferromagnetic phase transition near nominally nonmagnetic even filling factors [120, 121]. To estimate the strength of the electron-electron interaction in a magnetic field, it is reasonable to replace the Fermi energy with the distance between the Landau levels, which is also inversely proportional to the effective mass of the electrons. Strictly speaking, Landau quantization is valid only in the limit where the Coulomb repulsion is weak and can be considered a small correction.

Let us consider the phenomenon of the ferromagnetic phase transition near even filling factors in more detail, focusing on the behavior of the electron spin resonance near such a transition. As experimental samples, semiconductor heterostructures with a relatively large effective mass of $\sim 0.3-0.5\ m_0$, such as ZnO/MgZnO heterojunctions and AlAs quantum wells, are usually used. Such masses ensure the dominance of the Coulomb energy over the splitting between the Landau levels in typical magnetic fields. In Ref. [121], an analysis of the photoluminescence line shape of a two-dimensional electron system in ZnO/MgZnO heterojunctions made it possible to construct a phase diagram of the ferromagnetic transition near $\nu = 2$ in the following coordinates electron density–magnetic field tilt angle. Note that an increase in the magnetic field tilt angle leads to an increase in the spin splitting at a fixed filling factor of the electron system, since the filling factor is determined exclusively by the perpendicular component of the magnetic field, and the Zeeman splitting is determined by the total field. The higher the electron density and, therefore, the smaller the relative contribution from the exchange interaction, the greater the field tilt angle required for the transition of the electron system to a spin-polarized state. In Refs [120, 122], it was shown that such a transition is accompanied by the appearance of a clearly defined spike in the longitudinal resistance of the sample, which is apparently due to the division of the system into domains with different spin polarizations. In this case, the domain walls can scatter conduction electrons and lead to an increase in the resistance of the system. Such a spike is a very convenient indicator of a phase transition.

Let us now consider the evolution of the spin resonance near the ferromagnetic transition, measured in Ref. [123]. Figure 8 shows the longitudinal resistance of a two-dimensional electron system with a density of $n = 2.1 \times 10^{11}$ cm^{-2} at three different magnetic field tilt angles $\theta = 0°, 22.5°$, and $35°$ near a filling factor of 2. At an intermediate angle, a sharp peak is observed in the resistance, shown on a larger scale in Fig. 8b. Figure 8c shows a typical evolution of the spin resonance amplitude near an even filling factor. At zero tilt angle in the paramagnetic state, no spin resonance is observed, while at $\theta = 35°$ in the ferromagnetic state, ESR is observed in the entire range of fields in the vicinity of $\nu = 2$. At $\theta = 22.5°$, the resonance amplitude at a certain ν sharply decreases by several orders of magnitude, and the position of this drop coincides with the position of the peak in the resistance (labelled with a marker in the figure). Such behavior clearly indicates that near the peak in the resistance a ferromagnetic phase transition indeed occurs, accompanied by a macroscopic change in the spin polarization of the system. Moreover, in the same study, it was demonstrated that the shape of the ESR peak is significantly modified near the ferromagnetic transition — the spin resonance is split into several peaks. This is most likely associated with the appearance of domains with different spin polarizations. In this case, the possibility of scattering on domains actually leads to a violation of the Larmor theorem and much softer conditions on the law of conservation of the quasi-momentum of a spin wave.

Note that the behavior of the electron spin resonance in the nominally paramagnetic phase is also nontrivial. It is logical to expect that, in a state with zero spin moment, the phenomenon of electron spin resonance is not observed. This is precisely the behavior that was discovered near the ferromagnetic transition of the paramagnetic phase. However, if we try to measure the spin resonance in samples with a higher electron density and at a zero tilt angle — i.e., 'further' from the transition in the nominally nonmagnetic phase — it turns out that ESR is quite detectable, as was shown in Refs [124, 125]. Moreover, the spin resonance near an even filling factor has an important difference — its amplitude has a different sign from the resonance near odd filling factors. This fact is illustrated in Fig. 9a, b, which shows typical ESR

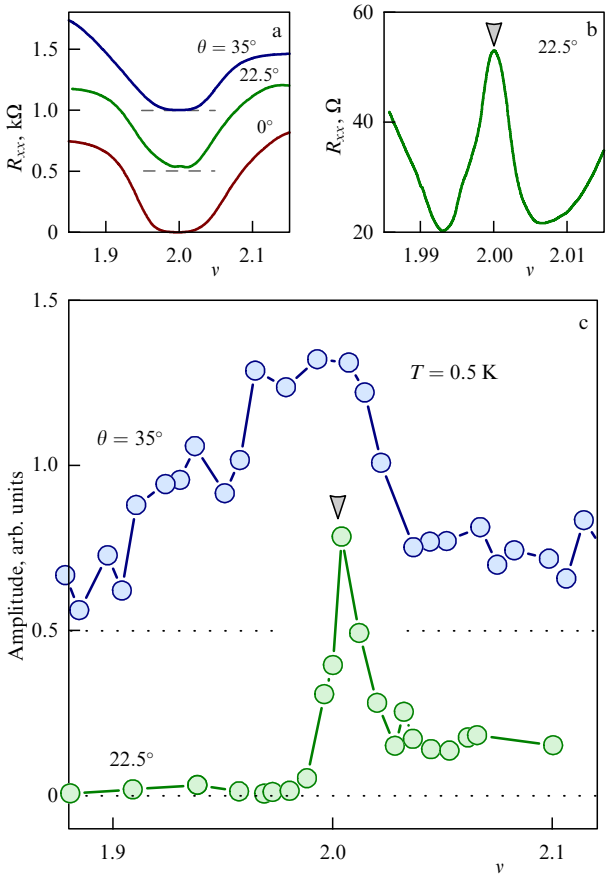

Figure 8. (a) Longitudinal resistance of a two-dimensional electron channel formed in a ZnO/MgZnO heterojunction at 0.5 K for three different magnetic field tilt angles $\theta = 0°$, 22.5°, and 35°. Two-dimensional electron density in sample was 2.1×10^{11} cm^{-2}. (b) Enlarged resistance of sample at $\theta = 22.5°$. Spike in resistance is pointed at with a marker. (c) Spin resonance amplitude measured in same sample as a function of filling factor for different magnetic field tilt angles. Marker points at position of peak in resistance associated with ferromagnetic phase transition at $\theta = 22.5°$.

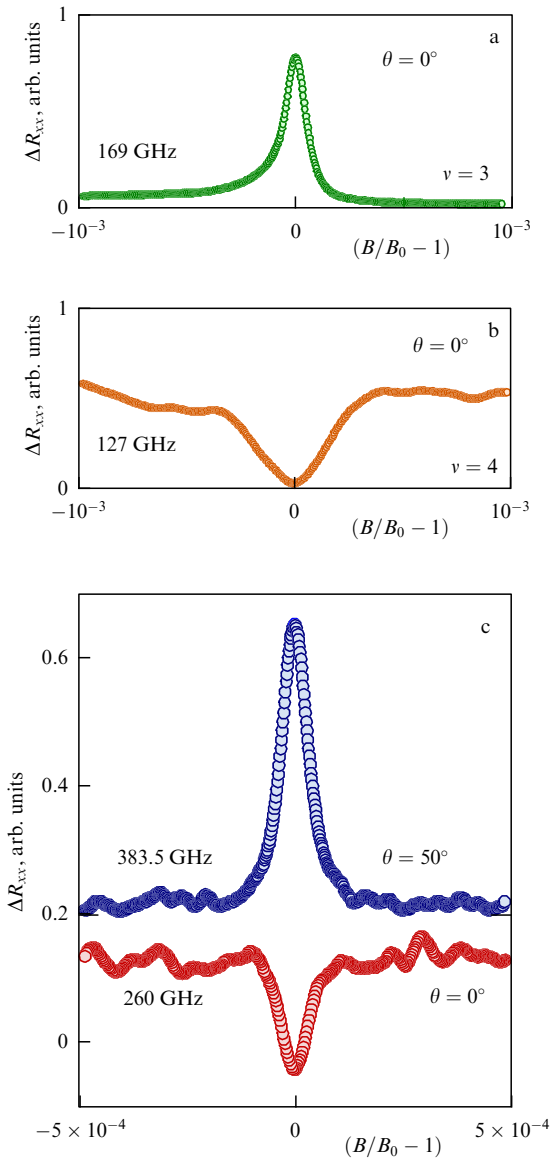

Figure 9. (a, b) Typical spin resonance peaks observed in a ZnO/MgZnO heterojunction with electron concentration $n = 4.5 \times 10^{11}$ cm^{-2} near filling factors of 3 and 4, respectively. Frequency of electromagnetic radiation is indicated in each of the two figures. Magnetic field is normalized to resonance value. Experimental temperature is 0.5 K. (c) Typical spin resonance peak measured near filling factor 2 in paramagnetic phase at $\theta = 0°$ and in ferromagnetic phase at 50°. Magnetic field is normalized to resonance value. Experimental temperature is 0.5 K.

peaks near filling factors 3 and 4, respectively, which were measured in a sample with a two-dimensional density of $n = 4.5 \times 10^{11}$ cm^{-2}.

The difference mentioned is of a fundamental nature. Indeed, near odd filling factors, the sign of the resistance change near the ESR corresponds to the heating of the electron system in full accordance with the mechanism discussed in one of the previous sections. However, near even filling factors, the spin resonance corresponds to a decrease in the resistance of the system, i.e., its 'cooling.' This feature was rechecked in [125] by directly measuring the resistance of the sample (i.e., without using the double lock-in amplifier technique). In the same study, it was shown that, upon a transition of the system to a ferromagnetic state near an even filling factor, the anomalous behavior of the spin resonance is also replaced by the usual 'heating' behavior. The data obtained allowed us to propose a hypothesis that describes all the main observed features of the spin resonance near even filling factors. The proposed explanation is based on the fact that, at a nonzero sample temperature and in not too high magnetic fields in the system near even filling factors, there is always a finite number of excitations, which can be thought of as a transition of an electron to the upper Landau level with a spin flip. Since both the Landau level number and the spin projection change in this case, the many-particle contribution to the energy of such modes is not forbidden. Moreover, as shown in Refs [5, 126, 127], their spectrum is softened due to electron-electron interaction. Since the excitation of such modes implies a spin flip, the system has a nonzero spin polarization, and electron spin resonance becomes possible. Under the action of microwave radiation, a redistribution of spin excitations probably occurs. This redistribution implies a decrease in the number of excitations with a large radius participating in dissipative charge transfer processes, and the resistance of the system decreases. When transitioning to the ferromagnetic state, the excitation spectrum changes — the spin exciton becomes the lowest, and the anomalous ESR mechanism is no longer valid. In

the immediate vicinity of the transition, domain nuclei effectively scatter the spin, significantly reduce the lifetime of spin excitations, and, as a result, make it impossible to observe electron spin resonance.

7. Conclusion

The study of electron spin in various semiconductor heterostructures is an important part of modern condensed matter physics. The presence of this internal degree of freedom significantly enriches the fundamental physics of such systems, giving rise to both unique ground states with a nontrivial structure and new excitations. From an applied point of view, the spin moment can be used in addition to the electron charge for storing and processing information, including in the paradigm of quantum computing.

The concept of a spin degree of freedom was formulated over a hundred years ago. The rapid development of spin physics since then has given rise to a variety of increasingly sophisticated techniques that allow studying the most subtle physical phenomena. One of the key experimental approaches to spin studies is the electron paramagnetic resonance technique, which has played a key role in the formation of physical concepts in a wide variety of areas. In particular, the ESR technique has proven to be extremely effective in studying the spin properties of two-dimensional electron systems.

The electron spin resonance technique is being continuously improved — the sensitivity of the method is increasing, and the operating range of electromagnetic radiation frequencies, magnetic fields, and temperatures is expanding. The techniques are being adapted to new and the most diverse structures. Thus, resonant absorption of microwave radiation, the frequency of which coincides with the spin splitting, is actively used to control the spin states of single electrons in quantum dots — in essence, spin qubits [128]. The possibility of detecting electron spin resonance in single-layer and multilayer graphene structures has recently been demonstrated [70, 72, 113, 129, 130]. The results of ESR spectroscopy [130], obtained in samples with layers misoriented relative to each other, will allow a better understanding of the nature of multiparticle effects arising in such structures, including superconductivity. Thus, the ESR technique remains relevant and in demand in the physics of low-dimensional semiconductor structures.

The study was supported by the Russian Science Foundation, grant no. 20-72-10097 (extension).

References

1. Koralek J D et al. *Nature* **458** 610 (2009)
2. Walser M et al. *Nature Phys.* **8** 757 (2012)
3. Stoner E C *Proc. R. Soc. London A* **165** 372 (1938) https://doi.org/10.1098/rspa.1938.0066
4. Drummond N D, Needs R J *Phys. Rev. Lett.* **102** 126402 (2009)
5. Kulik L V et al. *Phys. Rev. B* **72** 073304 (2005)
6. Fert A, Reyren N, Cros V *Nat. Rev. Mater.* **2** 17031 (2017)
7. Barrett S E et al. *Phys. Rev. Lett.* **74** 5112 (1995)
8. Bader S D, Parkin S S P *Annu. Rev. Condens. Matter Phys.* **1** 71 (2010)
9. Van Vleck J H *The Theory of Electric and Magnetic Susceptibilities* (Oxford: The Clarendon Press, 1932)
10. Stuart R, Marshall W *Phys. Rev.* **120** 353 (1960)
11. Ando T, Uemura Y *J. Phys. Soc. Jpn.* **37** 1044 (1974)
12. Falson J et al. *Nat. Mater.* **21** 311 (2022)
13. Shayegan M *Nat. Rev. Phys.* **4** 212 (2022)
14. Roth L M, Lax B, Zwerdling S *Phys. Rev.* **114** 90 (1959)
15. Ivchenko E L, Kiselev A A *Sov. Phys. Semicond.* **26** 827 (1992); *Fiz. Tekh. Poluprovodn.* **26** 1471 (1992)
16. Kalevich V K, Korenev V L *JETP Lett.* **57** 571 (1993); *Pis'ma Zh. Eksp. Teor. Fiz.* **57** 557 (1993)
17. Dresselhaus G *Phys. Rev.* **100** 580 (1955)
18. Bychkov Yu A, Rashba E I *JETP Lett.* **39** 78 (1984); *Pis'ma Zh. Eksp. Teor. Fiz.* **39** 66 (1984)
19. Datta S, Das B *Appl. Phys. Lett.* **56** 665 (1990)
20. Wu M W, Jiang J H, Weng M Q *Phys. Rep.* **493** 61 (2010)
21. Ivchenko E L *Phys. Usp.* **55** 808 (2012); *Usp. Fiz. Nauk* **182** 869 (2012)
22. Fu L, Kane C L *Phys. Rev. Lett.* **100** 096407 (2008)
23. Fu L, Kane C L *Phys. Rev. B* **79** 161408 (2009)
24. Urbaszek B et al. *Rev. Mod. Phys.* **85** 79 (2013)
25. Bechtold A et al. "Relaxation of electron and hole spin qubits in III–V quantum dots," in *Photonic Quantum Technologies: Science and Applications* (Ed. M Benyoucef) (New York: John Wiley Sons, 2023) p. 377, https://doi.org/10.1002/9783527837427.ch16
26. Gerlach W, Stern O *Z. Phys.* **8** 110 (1922)
27. Zavoysky E K "Paramagnitnaya absorbtsiya v perpendikulyarnykh i parallel'nykh polyakh dlya solei, rastvorov i metallov" ("Paramagnetic absorption in perpendicular and parallel fields for salts, solutions and metals"), Doctoral Thesis of Sci. in Phys. and Math. (Moscow: Lebedev Physical Institute, Academy of Sciences of the USSR, 1944)
28. Nestle N et al. *Phys. Rev. B* **56** R4359 (1997)
29. Weisbuch C, Hermann C *Phys. Rev. B* **15** 816 (1977)
30. Stein D, Klitzing K V, Weimann G *Phys. Rev. Lett.* **51** 130 (1983)
31. Poole C P (Jr.) *Electron Spin Resonance: a Comprehensive Treatise on Experimental Techniques* (Mineola, NY: Dover Publ., 1996)
32. Shchepetilnikov A V et al. *Appl. Phys. Lett.* **113** 052102 (2018)
33. Vasiliadou E et al. *Phys. Rev. B* **48** 17145 (1993)
34. Wei H P et al. *Phys. Rev. B* **32** 7016 (1985)
35. Engel L W et al. *Phys. Rev. Lett.* **71** 2638 (1993)
36. Khisameeva A R, Shchepetilnikov A V, Nefyodov Yu A, Kukushkin I V *Bull. Russ. Acad. Sci. Phys.* **85** 123 (2021); *Izv. Ross. Akad. Nauk. Fiz.* **85** 170 (2021)
37. Shchepetilnikov A V, Khisameeva A R, Nefyodov Yu A, Kukushkin I V *JETP Lett.* **110** 599 (2019); *Pis'ma Zh. Eksp. Teor. Fiz.* **110** 597 (2019)
38. Durkan C, Welland M E *Appl. Phys. Lett.* **80** 458 (2002)
39. Blick R H et al. *Phys. Rev. B* **57** R12685 (1998)
40. Meisels R et al. *Phys. Rev. B* **61** 5637 (2000)
41. Rashba E I, Sheka V I, in *Landau Level Spectroscopy* (Modern Problems in Condensed Matter Sciences, Vol. 27, Eds G Landwehr, E I Rashba) (Amsterdam: Elsevier, 1991) p. 131, https://doi.org/10.1016/B978-0-444-88535-7.50011-X
42. Gopalan S et al. *Phys. Rev. B* **34** 5466 (1986)
43. Duckheim M, Loss D *Nature Phys.* **2** 195 (2006)
44. Schulte M et al. *Phys. Rev. Lett.* **94** 137601 (2005)
45. Stier A V et al. *Phys. Rev. B* **107** 045301 (2023)
46. Chen Y-F et al. *Phys. Rev. B* **32** 890 (1985)
47. Bychkov Yu A, Iordanskii S V, Eliashberg G M *JETP Lett.* **33** 143 (1981); *Pis'ma Zh. Eksp. Teor. Fiz.* **33** 152 (1981)
48. Kallin C, Halperin B I *Phys. Rev. B* **30** 5655 (1984)
49. Shchepetilnikov A V et al. *JETP Lett.* **108** 481 (2018); *Pis'ma Zh. Eksp. Teor. Fiz.* **108** 516 (2018)
50. Pinczuk A et al. *Phys. Rev. Lett.* **68** 3623 (1992)
51. Kukushkin I V et al. *Appl. Phys. Lett.* **85** 4526 (2004)
52. Kukushkin I V et al. *Phys. Rev. Lett.* **96** 126807 (2006)
53. Nicholas R J et al. *Phys. Rev. B* **37** 1294 (1988)
54. Goldberg B B, Heiman D, Pinczuk A *Phys. Rev. Lett.* **63** 1102 (1989)
55. Dolgopolov V T et al. *Phys. Rev. Lett.* **79** 729 (1997)
56. Dickmann S, Ziman T *Phys. Rev. B* **85** 045318 (2012)
57. Zhuravlev A S et al. *Phys. Rev. B* **89** 161301 (2014)
58. Olshanetsky E et al. *Phys. Rev. B* **67** 165325 (2003)
59. Prati E et al. *IEEE Trans. Nanotechnol.* **4** 100 (2005)
60. Zhuravlev A S et al. *Phys. Rev. B* **77** 155404 (2008)
61. Khodaparast G A et al. *Physica E* **20** 386 (2004); in *Proc. of the 11th Intern. Conf. on Narrow Gap Semiconductors, NGS-11, 16–20 June 2003, Buffalo, NY, USA*

62. Nefyodov Yu A, Fortunatov A A, Shchepetilnikov A V, Kukushkin I V *JETP Lett*. **91** 357 (2010); *Pis'ma Zh. Eksp. Teor. Fiz*. **91** 385 (2010)
63. Dobers M, Klitzing K V, Weimann G *Phys. Rev. B* **38** 5453 (1988)
64. Lommer G, Malcher F, Rössler U *Phys. Rev. B* **32** 6965 (1985)
65. Sapega V F et al. *Phys. Rev. B* **50** 2510 (1994)
66. Eldridge P S et al. *Phys. Rev. B* **83** 041301 (2011)
67. Shchepetilnikov A V, Nefyodov Yu A, Kukushkin I V, Dietsche W *J. Phys. Conf. Ser*. **456** 012035 (2013)
68. Devizorova Zh A, Shchepetilnikov A V, Nefyodov Yu A, Volkov V A, Kukushkin I V *JETP Lett*. **100** 102 (2014); *Pis'ma Zh. Eksp. Teor. Fiz*. **100** 111 (2014)
69. Jiang H W, Yablonovitch E *Phys. Rev. B* **64** 041307 (2001)
70. Lyon T J et al. *Phys. Rev. Lett*. **119** 066802 (2017)
71. Anlauf T et al. *Phys. Rev. Materials* **5** 034006 (2021)
72. Sharma C H et al. *AIP Adv*. **12** 035111 (2022)
73. Ivchenko E L, Kiselev A A, Willander M *Solid State Commun*. **102** 375 (1997)
74. Kiselev A A, Ivchenko E L, Rössler U *Phys. Rev. B* **58** 16353 (1998)
75. Pfeffer P, Zawadzki W *Phys. Rev. B* **74** 233303 (2006)
76. Nefyodov Yu A, Shchepetilnikov A V, Kukushkin I V, Dietsche W, Schmult S *Phys. Rev. B* **83** 041307 (2011)
77. Nefyodov Yu A, Shchepetilnikov A V, Kukushkin I V, Dietsche W, Schmult S *Phys. Rev. B* **84** 233302 (2011)
78. Malinowski A, Harley R T *Phys. Rev. B* **62** 2051 (2000)
79. Hallstein S et al., in *High Magnetic Fields in the Physics of Semiconductors, Proc. of the 12th Intern. Conf., Würzburg, Germany, 29 July – 2 August 1996* (Eds G Landwehr, W Ossau) (Singapore: World Scientific, 1997) p. 593
80. Yugova I A et al. *Phys. Rev. B* **75** 245302 (2007)
81. Hannak R M et al. *Solid State Commun*. **93** 313 (1995)
82. Le Jeune P et al. *Semicond. Sci. Technol*. **12** 380 (1997)
83. Alekseev P S *JETP Lett*. **98** 84 (2013); *Pis'ma Zh. Eksp. Teor. Fiz*. **98** 92 (2013)
84. Ivchenko E L, Kaminski A Yu, Rössler U *Phys. Rev. B* **54** 5852 (1996)
85. Alekseev P S, Nestoklon M O *Phys. Rev. B* **95** 125303 (2017)
86. Alekseev P S, Nestoklon M O *Phys. Rev. B* **103** 195306 (2021)
87. Shchepetilnikov A V et al. *Phys. Rev. B* **92** 161301 (2015)
88. Tycko R et al. *Science* **268** 1460 (1995)
89. Tiemann L et al. *Science* **335** 828 (2012)
90. Overhauser A W *Phys. Rev*. **92** 411 (1953)
91. Dobers M et al. *Phys. Rev. Lett*. **61** 1650 (1988)
92. Abragam A, Goldman M *Rep. Prog. Phys*. **41** 395 (1978)
93. Berkovits V L et al. *Phys. Rev. B* **18** 1767 (1978)
94. Vitkalov S A et al. *Phys. Rev. B* **61** 5447 (2000)
95. Berg A et al. *Phys. Rev. Lett*. **64** 2563 (1990)
96. Shchepetilnikov A V et al. *Phys. Rev. B* **94** 241302 (2016)
97. Shchepetilnikov A V et al. *Phys. Rev. B* **96** 161301 (2017)
98. Hillman C, Jiang H W *Phys. Rev. B* **64** 201308 (2001)
99. Olshanetsky E et al. *Physica B* **373** 182 (2006)
100. Vitkalov S A e al. *J. Phys. Condens. Matter* **11** L407 (1999)
101. Vitkalov S A et al. *JETP Lett*. **69** 64 (1999); *Pis'ma Zh. Eksp. Teor. Fiz*. **69** 58 (1999)
102. Desrat W et al. *Physica E* **12** 149 (2002); in *Proc. of the Fourteenth Intern. Conf. on the Electronic Properties of Two-Dimensional Systems, EP2DS-14, 30 July – 3 August 2001, Praha, Czech Republic*
103. Desrat W et al. *Phys. Rev. Lett*. **88** 256807 (2002)
104. Stern M et al. *Phys. Rev. Lett*. **108** 066810 (2012)
105. Shchepetilnikov A V et al. *Phys. Rev. B* **98** 241302 (2018)
106. Shchepetilnikov A V et al. *Physica E* **124** 114278 (2020)
107. Shchepetilnikov A V, Khisameeva A R, Dremin A A, Kukushkin I V *JETP Lett*. **115** 548 (2022); *Pis'ma Zh. Eksp. Teor. Fiz*. **115** 595 (2022)
108. Larionov A V, Zhuravlev A S *JETP Lett*. **97** 137 (2013); *Pis'ma Zh. Eksp. Teor. Fiz*. **97** 156 (2013)
109. Shchepetilnikov A V et al. *Phys. Rev. Applied* **18** 024037 (2022)
110. Khisameeva A R, Shchepetilnikov A V, Dremin A A, Kukushkin I V *JETP Lett*. **117** 681 (2023); *Pis'ma Zh. Eksp. Teor. Fiz*. **117** 689 (2023)
111. Tsubaki K et al. *Appl. Phys. Lett*. **80** 3126 (2002)
112. Brosig S et al. *Phys. Rev. B* **60** R13989 (1999)
113. Sichau J et al. *Phys. Rev. Lett*. **122** 046403 (2019)
114. Krishtopenko S S *Semicond. Sci. Technol*. **29** 085005 (2014)
115. Krishtopenko S S, Gavrilenko V I, Goiran M *Phys. Rev. B* **87** 155113 (2013)
116. De Poortere E P et al. *Appl. Phys. Lett*. **80** 1583 (2002)
117. Tsukazaki A et al. *Nature Mater*. **9** 889 (2010)
118. Falson J et al. *Nature Phys*. **11** 347 (2015)
119. Kukushkin I V et al. *Phys. Rev. Lett*. **72** 3594 (1994)
120. Kozuka Y et al. *Phys. Rev. B* **85** 075302 (2012)
121. Van'kov A B, Kaysin B D, Kukushkin I V *Phys. Rev. B* **96** 235401 (2017)
122. De Poortere E P, Tutuc E, Shayegan M *Phys. Rev. Lett*. **91** 216802 (2003)
123. Shchepetilnikov A V, Khisameeva A R, Nefyodov Yu A, Kukushkin I V *JETP Lett*. **113** 657 (2021); *Pis'ma Zh. Eksp. Teor. Fiz*. **113** 689 (2021)
124. Shchepetilnikov A V, Khisameeva A R, Nefyodov Yu A, Kukushkin I V *Phys. Rev. B* **104** 075437 (2021)
125. Shchepetilnikov A V, Khisameeva A R, Nikolaev G A, Lopatina S A, Kukushkin I V *Phys. Rev. B* **107** 195415 (2023)
126. Dickmann S, Kukushkin I V *Phys. Rev. B* **71** 241310 (2005)
127. Dickmann S, Kaysin B D *Phys. Rev. B* **101** 235317 (2020)
128. Burkard G et al. *Rev. Mod. Phys*. **95** 025003 (2023)
129. Prada M et al. *Phys. Rev. B* **104** 075401 (2021)
130. Lin J-X et al. *Science* **375** 437 (2022)